# Strong green photoluminescence from $In_xGa_{1-x}N$/GaN nanorod arrays

**Chi-Chang Hong,[1] Hyeyoung Ahn[1,*], Chen-Ying Wu,[2] and Shangjr Gwo[2]**

[1]*Department of Photonics and Institute of Electro-Optical Engineering, National Chiao Tung University, Hsinchu, Taiwan 30010, Republic of China*

[2] *Department of Physics, National Tsing Hua University, Hsinchu, Taiwan 30013, Republic of China*

** hyahn@mail.nctu.edu.tw*

**Abstract:** We report intense green photoluminescence (PL) from vertically aligned indium gallium nitride ($In_xGa_{1-x}N$) nanorod arrays. The formation of $In_xGa_{1-x}N$/GaN-heterostructure nanorods increases the localization depth of the radially confined carriers (> 100 meV). Temperature dependent PL peak energy of InGaN nanorods shows the characteristic S-shaped behavior, indicating the prominent carrier trapping in band-tail states associated with the nonuniformity of In content. Time-resolved PL (TRPL) response decays biexponentially and the dominant slow decay component of TRPL for $In_xGa_{1-x}N$ nanorods is due to the transfer of excitons to the localized states before the radiative decay.



**OCIS codes:** (160.4236) Nanomaterials; (160.6000) Semiconductor materials; (250.5230) Photoluminescence; (300.6280) Spectroscopy, fluorescence and luminescence.

## References and links

1. H. Morkoç, and S. N. Mohammad, "High-luminosity blue and blue-green gallium nitride light-emitting diodes," Science **267**(5194), 51–55 (1995).
2. F. A. Ponce, and D. P. Bour, "Nitride-based semiconductors for blue and green light-emitting devices," Nature **386**(6623), 351–359 (1997).
3. S. Nakamura, and G. Fasol, *The Blue Laser Diode* (Springer, New York, 1997).
4. M. Yoshizawa, A. Kikuchi, M. Mori, N. Fujita, and K. Kishino, "Growth of self-organized GaN nanostructures on $Al_2O_3$(0001) by RF-radical source molecular beam epitaxy," Jpn. J. Appl. Phys. **36**(Part 2, No. 4B), L459–L462 (1997).
5. E. Calleja, M. A. Sánchez-García, F. J. Sánchez, F. Calle, F. B. Naranjo, E. Muñoz, U. Jahn, and K. Ploog, "Luminescence properties and defects in GaN nanocolumns grown by molecular beam epitaxy," Phys. Rev. B **62**(24), 16826–16834 (2000).
6. Y. S. Park, C. M. Park, D. J. Fu, T. W. Kang, and J. E. Oh, "Photoluminescence studies of GaN nanorods on Si (111) substrates grown by molecular-beam epitaxy," Appl. Phys. Lett. **85**(23), 5718 (2004).
7. H.-M. Kim, Y.-H. Cho, H. Lee, S. I. Kim, S. R. Ryu, D. Y. Kim, T. W. Kang, and K. S. Chung, "High-brightness light emitting diodes using dislocation-free indium gallium nitride/gallium nitride multiquantum-well nanorod arrays," Nano Lett. **4**(6), 1059–1062 (2004).
8. C. H. Chiu, T. C. Lu, H. W. Huang, C. F. Lai, C. C. Kao, J. T. Chu, C. C. Yu, H. C. Kuo, S. C. Wang, C. F. Lin, and T. H. Hsueh, "Fabrication of InGaN/GaN nanorod light-emitting diodes with self-assembled Ni metal islands," Nanotechnology **18**(44), 445201 (2007).
9. Y. Kawakami, S. Suzuki, A. Kaneta, M. Funato, A. Kikuchi, and K. Kishino, "Origin of high oscillator strength in green-emitting InGaN/GaN nanocolumns," Appl. Phys. Lett. **89**(16), 163124 (2006).
10. H.-Y. Chen, H.-W. Lin, C.-H. Shen, and S. Gwo, "Structure and photoluminescence properties of epitaxially oriented GaN nanorods grown on Si (111) by plasma-assisted molecular-beam epitaxy," Appl. Phys. Lett. **89**(24), 243105 (2006).
11. H.-S. Chen, D.-M. Yeh, Y.-C. Lu, C.-Y. Chen, C.-F. Huang, T.-Y. Tang, C. C. Yang, C.-S. Wu, and C.-D. Chen, "Strain relaxation and quantum confinement in InGaN/GaN nanoposts," Nanotechnology **17**(5), 1454–1458 (2006).
12. H.-Y. Chen, H.-W. Lin, C.-Y. Wu, W.-C. Chen, J.-S. Chen, and S. Gwo, "Gallium nitride nanorod arrays as low-refractive-index transparent media in the entire visible spectral region," Opt. Express **16**(11), 8106–8116 (2008).
13. S. Gwo, C.-L. Wu, C.-H. Shen, W.-H. Chang, T. M. Hsu, J.-S. Wang, and J.-T. Hsu, "Heteroepitaxial growth of wurtzite InN films on Si(111) exhibiting strong near-infrared photoluminescence at room temperature," Appl. Phys. Lett. **84**(19), 3765 (2004).
14. A. R. Denton, and N. W. Ashcroft, "Vegard's law," Phys. Rev. A **43**(6), 3161–3164 (1991).
15. P. G. Eliseev, P. Perlin, J. Lee, and M. Osinski, "Blue temperature-induced shift and band-tail emission in InGaN-based light sources," Appl. Phys. Lett. **71**(5), 569 (1997).

#111104 - $15.00 USD Received 12 May 2009; revised 2 Aug 2009; accepted 3 Aug 2009; published 14 Sep 2009

P. G. Eliseev, M. Osinski, J. Lee, T. Sugahara, and S. Sakai, "Band-tail model and temperature-induced blue-shift in photoluminescence spectra of $In_xGa_{1-x}N$ grown on sapphire," J. Electron. Mater. **29**(3), 332–341 (2000).
16. Y. H. Cho, G. H. Gainer, A. J. Fischer, J. J. Song, S. Keller, U. K. Mishra, and S. P. DenBaars, "S-shaped temperature-dependent emission shift and carrier dynamics in InGaN/GaN multiple quantum wells," Appl. Phys. Lett. **73**(10), 1370 (1998).
17. H.-S. Chang, T.-M. Hsu, T.-F. Chuang, W.-Y. Chen, S. Gwo, and C.-H. Shen, "Localized states in $In_xGa_{1-x}N$ epitaxial film," Solid State Commun. **149**(1-2), 18–20 (2009).
18. S. Nakamura, and S. F. Chichibu, *Introduction to Nitride Semiconductor Blue Lasers and Light Emitting Diodes* (Taylor & Francis, 2000), Chap. 5.
19. R. C. Miller, D. A. Kleinman, W. A. Nordland, Jr., and A. C. Gossard, "Luminescence studies of optically pumped quantum wells in GaAs-$Al_xGa_{1-x}As$ multilayer structures," Phys. Rev. B **22**(2), 863–871 (1980).
20. R. J. Archer, "Materials for light emitting diodes," J. Electron. Mater. **1**(1), 127–153 (1972).
21. Y. Narukawa, Y. Kawakami, and S. Fujita, "Dimensionality of excitons in laser-diode structures composed of $In_xGa_{1-x}N$ multiple quantum wells," Phys. Rev. B **59**(15), 10283–10288 (1999).

## 1. Introduction

InGaN-based semiconductors have attracted much attention for their applications as bright light emitting sources, such as light emitting devices (LEDs) and laser diodes (LDs) in the visible and UV spectral regions [1–3]. The bright III-nitride LEDs and LDs are typically realized on III-nitride compounds consisting of single quantum well (SQW) or multiple QW (MQW) structures since QW-active layers can reduce the carrier capturing in nonradiative defects and improve the light emission efficiency. For these planar type structures, it has been well-known that the quantum confined Stark effect (QCSE) induced by the piezoelectric field and high density of defects, resulting from a large lattice mismatch between InGaN and GaN, limit the performance of InGaN QW devices. Especially the external quantum efficiency of currently available InGaN-QW devices drastically drops beyond the green spectral range. Recently it has been reported that dislocation- and strain-free group-III nitrides can be obtained by forming one-dimensional structures, such as nanocolumns or nanorods [4–6]. Moreover, InGaN-QW nanorod heterostructures have also been fabricated and light emission enhancement due to the carrier confinement and strain-relaxation effects has been observed [7–11]. Therefore, the absence of QCSE effects is highly anticipated in InGaN/GaN nanorod heterostructures.

In this work, to fully suppress the QW structure-induced piezoelectric field, we fabricated the InGaN/GaN nanorods without embedded QW-active layers by plasma-assisted molecular-beam epitaxy (PA-MBE) and investigated their emission processes. From the photoluminescence (PL) measurement from InGaN nanorods and film, we found that vertically-aligned $In_{0.11}Ga_{0.89}N$/GaN-heterostructure nanorods can emit about one order of magnitude stronger green light than that of an $In_{0.13}Ga_{0.87}N$ film counterpart. Temperature dependent PL spectra of InGaN/GaN nanorods show the pronounced S-shaped behavior, which indicates a high density localized states within the band-tails. The localization depth of nanorods estimated from the time-resolved PL (TRPL) responses is much larger than that of the film counterpart and the carrier localization of InGaN nanorods is mainly associated with the increase of In composition nonuniformity in nanorods. In addition to the increased effect of carrier localization, the large surface area of nanorods increases the light extraction efficiency and the low effective refractive index [12] reported for the group-III nitride nanorods could also contribute to the enhancement of PL emission.

## 2. Experimental methods

The vertically aligned InGaN/GaN nanorod arrays were grown on β-$Si_3N_4$/Si(111) by PA-MBE [13] under nitrogen-rich conditions with respect to the nitrogen flux used for film growth. First the GaN nanorod arrays (~380 nm) were grown at sample temperature of 760°C on β-$Si_3N_4$/Si(111). Then, the InGaN nanorods (~300 nm) were continuously grown on top of GaN nanorods to form the InGaN/GaN heterostructure at sample temperature of 700°C. The N/Ga and N/Ga/In flux ratios were 11:5 and 36:6:1 for GaN and InGaN nanorods, respectively. And the crystal polarities of GaN and InGaN nanorods were determined to be N-polar. X-ray diffraction (XRD) analysis shows that both InGaN film and nanorod arrays

#111104 - $15.00 USD Received 12 May 2009; revised 2 Aug 2009; accepted 3 Aug 2009; published 14 Sep 2009

have the wurtzite lattice structure and the X-ray peak of InGaN nanorods has the full-width-half-maximum (FWHM) close to that of the InGaN film. From the X-ray peak positions, the *c*-axis lattice constants of the sample were estimated. Using the Vegard's law [14], the In composition of InGaN nanorods was determined to be around 11%, whereas that of InGaN film is about 13%. The morphology and size distribution of InGaN/GaN nanorods were analyzed using field-emission scanning electron microscopy (FE-SEM). The FE-SEM images of the top- and side-view of hexagonal-shaped InGaN/GaN nanorod arrays in Fig. 1(a) and (b) show that the nanorods with an average radius of 30 ± 4 nm are vertically well aligned and have homogeneous length and diameter distributions. Meanwhile, Fig. 1(a) exhibits that the nanorod arrays are in fact composed of coalesced nanorod bundles instead of individually separated single nanorod, which has also been observed for the case of GaN nanorods [12]. The total length of nanorods consisted of InGaN (~300 nm) and GaN heterostructure is ~680 nm.

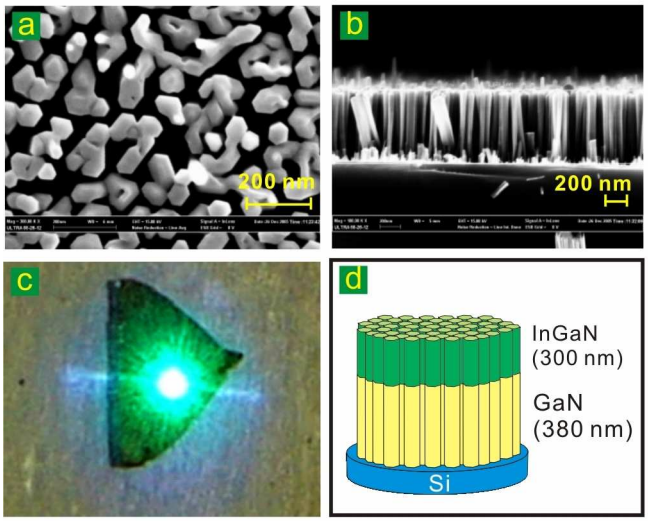


Fig. 1. FE-SEM images of top- (a) and side-view (b) of InGaN/GaN nanorods. The coalesced nanorod bundles composed of three to four nanorods can be observed. (c) A photograph of room-temperature PL from InGaN/GaN nanorods taken with a green color filter. (d) Layer structure of InGaN/GaN-heterostructure nanorods grown on top of a Si(111) substrate.

For both time-integrated and time-resolved PL analyses, the samples were photoexcited by the normally incident femtosecond laser pulses. A Ti:sapphire femtosecond laser system delivers ~150 fs laser pulses at the repetition rate of 82 MHz with the center wavelength of 800 nm. The pump laser pulses with the wavelength of 400 nm were obtained by a second harmonic generation crystal and the power of pump pulses were kept at 5 mW for whole PL measurements. The temperature dependence of PL spectra was measured at the sample temperature ranging from 4 to 300 K by a 1/4-m spectrometer equipped with a 600 g/mm grating and a liquid-nitrogen-cooled charge-coupled-device detector. All of the PL spectra have been corrected by the system response curve. The temporal evolution of the PL signals at different sample temperatures and PL peak positions were measured by a time-correlated single photon counting (TCSPC) system and the typical time resolution of our TCSPC system is approximately 180 ps.

### 3. Results and discussion

Figure 2 shows the normalized PL spectra of the InGaN film and nanorod arrays measured at 10 K. The PL peak energies of the film and nanorods are located at 2.42 and 2.32 eV and the bandwidths are 0.24 and 0.17 eV, respectively. The significant shift of PL peak energy (~100 meV) to longer wavelength for the nanorods is very different from the spectral shift of InGaN-

#111104 - $15.00 USD Received 12 May 2009; revised 2 Aug 2009; accepted 3 Aug 2009; published 14 Sep 2009

QW nanostructures which typically shows the blueshift and would reduce the merit of the formation of nanostructure for the generation of intense green emission. The bandwidth of 0.17 eV for InGaN nanorods is comparable [11] or narrower than those of nanocolumns of the InGaN/GaN-QW structure [9]. The observed narrow bandwidth of PL for our nanorods may be attributed to the reduction of lattice mismatch during the epitaxial growth of InGaN/GaN-heterostructure nanorods since most of the structural defects might only occur at the GaN-nanorods/substrate interface. More importantly, Fig. 2 exhibits that the PL intensity of InGaN/GaN nanorods is about 15 times stronger than that of the InGaN film. The emitted green light from nanorods was so bright that even the room-temperature emission could be clearly seen with the naked eyes under the room light. [see Fig. 1(c)].

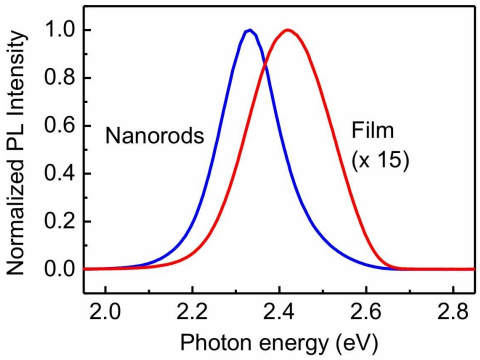


Fig. 2. Normalized PL spectra of the InGaN film and nanorods. The PL intensity of the InGaN film is about 15 times smaller than that of the InGaN nanorods.

Figure 3 shows the temperature-dependent PL response for InGaN nanorods. The figure exhibits that the PL peak energy of the InGaN nanorods shows an apparent S-shaped dependence on temperature. With increasing temperature up to 160 K, the PL peak energy initially blueshifts and at higher temperatures it gradually redshifts, following the temperature dependence described by Varshni's equation. It is well known that the S-shaped temperature-induced blueshift of emission peak of InGaN is due to the presence of deeply confined localized states within the tail density of states. Then the emission peak energies have the temperature dependence as given by [15]

$$h\nu_0 = E_0(T) - \sigma^2 / k_B T \qquad (1)$$

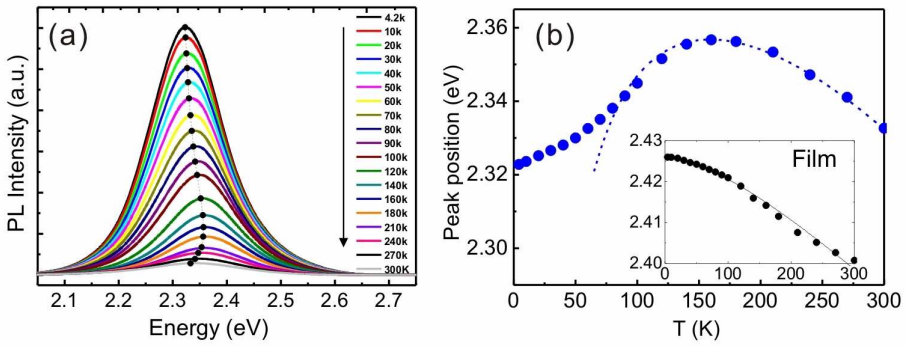


Fig. 3. Temperature-dependent PL spectra (a) and the PL peak energy (b) of InGaN/GaN nanorods. The temperature dependence of PL peak position shows a characteristic blueshift at low temperature range. The dashed line was obtained by Eq. (1) in the text.

where $k_B$ is Boltzmann's constant, $\sigma$ is the characteristic parameters describing the shape of the energy band-tail. The initial blueshift followed by the redshift of InGaN nanorods are well

#111104 - $15.00 USD Received 12 May 2009; revised 2 Aug 2009; accepted 3 Aug 2009; published 14 Sep 2009

described by Eq. (1) with the corresponding fit parameters of $\sigma$ = 22.1 meV, $E_0$ = 2.3 eV. Similar S-shape behavior has been reported previously for III-nitride ternary or QW system [6,16] and InGaN film with high In concentration (> 30%) [17]. The estimated tail parameter $\sigma$ = 22 meV is in a good agreement with those observed for InGaN/GaN quantum well nanostructures (~30 meV) [16]. Meanwhile, for our InGaN film a weak blueshift immediately followed by a redshift was observed. (see the inset in Fig. 3) This result shows that the one-dimensional structure of nanorods affects the PL behavior and it may be due to the confinement of carriers in small volume of nanorods.

TRPL spectroscopy has been performed at various temperatures and the results are shown in Fig. 4. At low temperature, the initial PL transient of InGaN nanorods reaches the maximum value at a delayed time ~500 ps whereas that of film reaches its maximum instantaneously after excitation pulse arrives (not shown). The delayed maximum emission of nanorods indicates that mobile excitons in deeper localized states within the local potential minima takes a certain delayed time to reach the states with maximum localization depth [18]. At each temperature, the PL responses of InGaN nanorods are expressed by a double exponential curve, $I(t) = I_1 e^{-t/\tau_1} + I_2 e^{-t/\tau_2}$, where $I_1$ and $I_2$ and $\tau_1$ and $\tau_2$ represent the PL intensities and decay time constants of the fast and slow components, respectively. The decay times of InGaN nanorods decrease from 1.5 (5.5) to 0.6 (3.3) ps for the fast and slow decay components, respectively, when the temperature increases from 10 to 300 K, implying the increase of non-radiative recombination at elevated temperatures. The decay times of InGaN/GaN nanorods are slower than those of InGaN films and it may be because the excitons in the nanorods are deeply localized and they can hardly reach impurity and defect centers before radiative recombination even at high temperature. The PL spectrum and spectral lifetimes of InGaN/GaN nanorods are summarized in Fig. 4(b). The wavelength dependence of the decay times indicates that the PL decay time decreases as the emission energy increases. According to the recombination dynamics of localized excitons, the lifetime of PL spectrum for above-bandgap excitation can be fitted by

$$\tau_{1,2}(E) = \frac{\tau_{\mathrm{rad}}}{1+\exp[(E-E_{\mathrm{me}})/E_{\mathrm{loc}}]}, \qquad (2)$$

where $\tau_{\mathrm{rad}}$ is the radiative lifetime, $E_{\mathrm{me}}$ is the energy of the mobility edge, and $E_{\mathrm{loc}}$ represents the localization depth. Solid lines in Fig. 4(b) are obtained from the best fitting to the measured data using Eq. (2) with $E_{\mathrm{loc}}$ of 102 and 139 meV, $\tau_{\mathrm{rad}}$ of 1.5 and 5.6 ns for the fast and slow decay components, respectively. The large values of $E_{\mathrm{loc}}$ of nanorods compared to that of film (30–40 meV) confirm the fact that excitons in the nanorods are strongly localized in the band tail states.

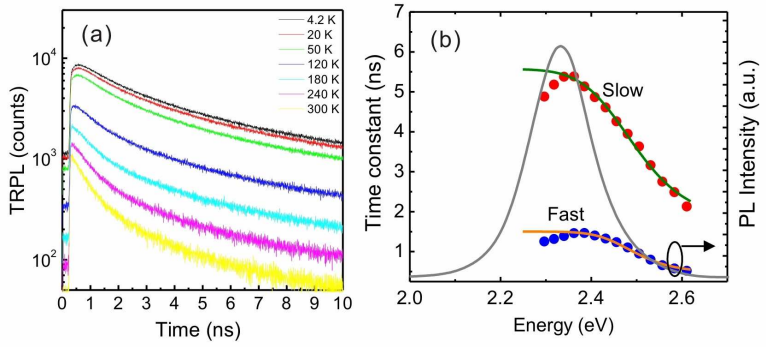


Fig. 4. (a) TRPL responses at different sample temperatures. (b) Fast and slow decay time constants are shown with the PL spectra. The solid lines are obtained by using Eq. (2).

#111104 - $15.00 USD Received 12 May 2009; revised 2 Aug 2009; accepted 3 Aug 2009; published 14 Sep 2009

In general, exciton localization in $In_xGa_{1-x}N$ system can be introduced by the nonuniformity of alloy composition, such as the In content in the form of In-rich clusters. In $In_xGa_{1-x}N$ system, the increase of InN molecular fraction $x$ increases the effective localization depth, which in return enhances the radiative recombination of localized excitons. However, at the same time, relatively fast increase of the density of nonradiative defects with increasing $x$ hampers the net enhancement of emission from InGaN with large $x$. For our $In_xGa_{1-x}N$ nanorod samples, the In composition of InGaN nanorods is lower than that of the film so that the increase of localization depth would not increase the nonradiative defect centers, but effectively enhance radiative recombination. Due to the variation of InGaN bandgap with the In composition, higher In composition typically induces the redshift of PL peak for $In_xGa_{1-x}N$ compounds. Our results, however, demonstrate that strong carrier localization due to the increase of In composition nonuniformity in nanorods can be obtained through the self-assembled growth of nanostructures without significantly increasing $x$. Therefore, the redshift of PL peak occurs due to this strong carrier localization phenomenon even when the In composition of InGaN nanorods is lower than the film counterpart, as shown in Fig. 2. Meanwhile, since the strong localization in InGaN nanorods is limited to a small volume within a nm-scale spatial range, carrier localization in nanorods corresponds to deeply confined localization. A recent micro-PL study on high-In-content InGaN compound [17] revealed that the deeply confined localization states induce the sharp spectral lines in the PL spectra, while the extended shallow localized states form the background profile of PL spectra. Therefore, the PL spectral width of InGaN nanorods may still depend on the In composition and crystal quality of InGaN nanorods. As a result, the observed PL linewidth of the nanorod sample is narrower than the film counterpart.

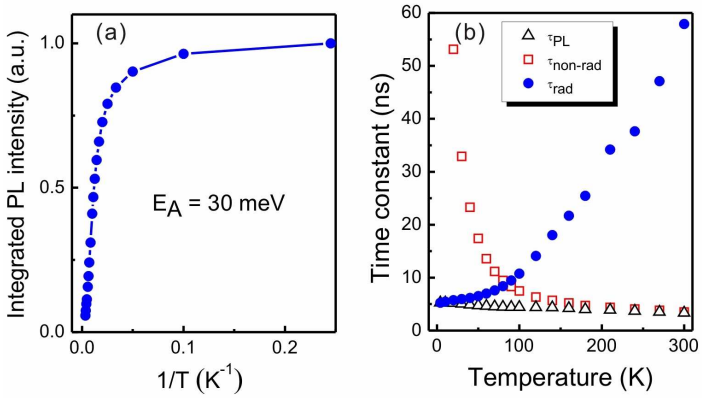


Fig. 5. (a) Intensity variation of the PL intensity as a function of reciprocal temperature for InGaN nanorods. The activation energy is about 30 meV and the deduced internal quantum efficiency can reach 6.3%. (b) PL lifetime $\tau_{PL}$ of InGaN nanorods with $\tau_{rad}$ and $\tau_{non\text{-}rad}$ as a function of $T$.

The internal quantum efficiency η in the InGaN/GaN nanorods was obtained from the Arrhenius plot of the normalized PL intensity as shown in Fig. 5(a). From the slope of the straight line at high temperature range, the activation energy was determined to be 30 meV. About 6.3% of the internal quantum efficiency at room temperature was estimated from the relation of $I$(300 K)/$I$(20 K) of InGaN nanorods, indicating a high PL efficiency even at room temperature. Radiative ($\tau_{rad}$) and nonradiative ($\tau_{non\text{-}rad}$) lifetime at $T$ are related with the PL decay time ($\tau_{PL}$) and η by the following equations [19,20]:

$$\tau_{rad}(T) = \frac{\tau_{PL}(T)}{\eta(T)}, \quad \tau_{non-rad}(T) = \frac{\tau_{PL}(T)}{1-\eta(T)}. \tag{3}$$

Figure 5(b) shows temperature dependence of $\tau_{PL}(T)$, $\tau_{rad}(T)$, and $\tau_{non\text{-}rad}(T)$ of InGaN nanorods. The $\tau_{rad}$ values increase linearly for temperature up to ~100 K with the slope of 30

#111104 - $15.00 USD Received 12 May 2009; revised 2 Aug 2009; accepted 3 Aug 2009; published 14 Sep 2009

$psK^{-1}$. This linear dependence of $\tau_{rad}$ on $T$ represents the low-dimensional feature of excitons, corresponding to exciton localization at potential minima at low temperatures [21]. At higher temperatures, most of the carriers recombine through nonradiative channels.

In addition to the increase carrier localization due to the formation of nanostructures, the sidewalls of nanorods can increase the surface area for effective absorption of pump light and green light emission. The low effective refractive index and reduced loss from total internal reflection [12] can also contribute to the enhancement of luminescence from our InGaN/GaN nanorod arrays. Although it is difficult to quantitatively estimate the contribution of geometrical effect of nanorods, less than five times of enhancement in PL intensity has been reported for InGaN nanostructures fabricated by bottom-up or top-down methods [7–9].

## 4. Summary

In summary, we have demonstrated that $In_xGa_{1-x}N$/GaN-heterostructure nanorod arrays with the rod radial size of ~30 nm can radiate intense green luminescence. Temperature-dependent PL peak energy of $In_xGa_{1-x}N$/GaN nanorods shows the distinctive S-shape dependence and it is attributed to the formation of band-tail states associated with strong carrier localization effects. It was confirmed by the large value of localization depth deduced from TRPL measurement. The enhancement of the green light emission from epitaxially-grown InGaN nanorods is due to the radiative recombination of deeply localized excitions associated with the increased composition non-uniformity in the nanorods.

## Acknowledgement

This work was supported by the National Science Council (NSC) in Taiwan through several grants, including NSC 98-2112-M-009-009-MY3 and the National Nanoscience and Nanotechnology Project (NSC 98-2120-M-007-009).

#111104 - $15.00 USD Received 12 May 2009; revised 2 Aug 2009; accepted 3 Aug 2009; published 14 Sep 2009